



December 2002

Nanoimpedance Microscopy and Spectroscopy

Rui Shao

University of Pennsylvania, rshao@seas.upenn.edu

Sergei V. Kalinin

Oak Ridge National Laboratory

Dawn A. Bonnell

University of Pennsylvania, bonnell@lrsm.upenn.edu

Follow this and additional works at: http://repository.upenn.edu/mse_papers

Recommended Citation

Shao, R., Kalinin, S. V., & Bonnell, D. A. (2002). Nanoimpedance Microscopy and Spectroscopy. Retrieved from http://repository.upenn.edu/mse_papers/28

Copyright Materials Research Society. Reprinted from MRS Proceedings Volume 738.

2002 Fall Meeting Symposium G

Spatially Resolved Characterization of Local Phenomena in Materials and Nanostructures

Publisher URL: http://www.mrs.org/members/proceedings/fall2002/g/G4_4.pdf

This paper is posted at ScholarlyCommons. http://repository.upenn.edu/mse_papers/28

For more information, please contact libraryrepository@pobox.upenn.edu.

Nanoimpedance Microscopy and Spectroscopy

Abstract

One of the key limiting factors in current-based scanning probe microscopies (SPM) is the quality of tip-sample contact and stray capacitance in the probe-surface junction. We conduct impedance spectroscopy over a broad frequency range (40Hz~110MHz) through an AFM tip to quantify local electrical properties. Equivalent circuit for the tip-surface contact is constructed based on the impedance data and is used to study the mechanisms of relaxation in the near-tip region. Relative contributions of tip-surface contact and materials properties to the signal are discussed. This technique, referred to as Nanoimpedance Microscopy/Spectroscopy, is demonstrated in the imaging of an electronic ceramic: a ZnO varistor. Analysis of impedance spectra allows separation of tip-surface interactions and grain boundary behavior.

Comments

Copyright Materials Research Society. Reprinted from MRS Proceedings Volume 738.

2002 Fall Meeting Symposium G

Spatially Resolved Characterization of Local Phenomena in Materials and Nanostructures

Publisher URL: http://www.mrs.org/members/proceedings/fall2002/g/G4_4.pdf

NANOIMPEDANCE MICROSCOPY AND SPECTROSCOPY

Rui Shao, *Sergei V. Kalinin, and Dawn A. Bonnell

Department of Materials Science and Engineering, University of Pennsylvania
3231 Walnut St, Philadelphia, PA 19104

ABSTRACT

One of the key limiting factors in current-based scanning probe microscopies (SPM) is the quality of tip-sample contact and stray capacitance in the probe-surface junction. We conduct impedance spectroscopy over a broad frequency range (40Hz~110MHz) through an AFM tip to quantify local electrical properties. Equivalent circuit for the tip-surface contact is constructed based on the impedance data and is used to study the mechanisms of relaxation in the near-tip region. Relative contributions of tip-surface contact and materials properties to the signal are discussed. This technique, referred to as Nanoimpedance Microscopy/Spectroscopy, is demonstrated in the imaging of an electronic ceramic: a ZnO varistor. Analysis of impedance spectra allows separation of tip-surface interactions and grain boundary behavior.

INTRODUCTION

The continuous miniaturization of integrated electrical devices and growing interest in submicron phenomena require reliable methods to characterize local electrical properties. Recently, many scanning probe microscopy (SPM) techniques based on contact mode AFM have been developed. They are implemented either by current or capacitance sensing via a nanoscale sharp AFM tip in contact with the sample surface [1-3]. One of the most significant factors affecting these SPM techniques is tip-surface contact.

Here, we have applied impedance spectroscopy to the characterization of the contact between an AFM tip and a flat noble metal surface in order to determine electrical parameters of tip-surface junction, such as stray capacitance, contact resistance of different conductive coatings, inductance and the dc bias dependence of these parameters.

The measurement of the frequency dependence of ceramic or semiconductor samples using a conductive tip is implemented and referred to as Nanoimpedance Microscopy/Spectroscopy (NIM). If contact resistance is small, the measured capacitance is due to relatively large microstructural elements, such as grain boundaries, etc, as demonstrated by impedance imaging and spectroscopy of a polycrystalline ZnO.

THEORY

Impedance Z is defined as the ratio of ac bias applied to the system, V_{ac} to the current response, I_{ac} , as $Z(\omega)=V_{ac}/I_{ac}$, where V_{ac} , I_{ac} are in complex form and ω is frequency. In general, $Z = Z_r+i \cdot Z_i=|Z|exp(i\theta)$, where Z_r , Z_i are the real and imaginary parts of Z , and $|Z|$, and θ are the modulus and phase of Z . The impedance, Z of an ideal resistor, R , is $Z = R$,

* Currently at Condensed Matter Sciences Division, Oak Ridge National Laboratory

$\theta = 0^\circ$; for an ideal capacitor, C , $Z=1/(i\omega C)$, $\theta=-90^\circ$; for an ideal inductor, L , $Z=i\omega L$, $\theta=+90^\circ$.

The system of a tip in contact with a metal surface is best modeled by a parallel R-C element corresponding to the tip-surface resistance in parallel with probe-surface capacitance. The cable inductance results in an additional serial inductive element. Measurement of frequency-dependent impedance allows unambiguous separation of these quantities (impedance spectroscopy [4]). This method is applied to investigate several commercially available AFM tips with different conductive coatings. Parameters of the equivalent circuit are determined by complex nonlinear fitting.

AFM impedance spectra on polycrystalline materials exhibit the fingerprints of several relaxation processes, such as tip/sample contact, grain boundary, grain bulk and circuit inductance which can be differentiated according to characteristic time constants [4].

EXPERIMENTAL DETAILS

AFM based impedance spectroscopy and imaging, were carried out on a commercial AFM system (DI Dimension 3000 NS IIIA). Impedance amplitude and phase, $|Z|/\theta$, were collected by an impedance analyzer HP4294A over the frequency range of 40Hz to 110MHz. The AFM tip is electrically connected to the impedance analyzer through a custom-built tip holder. The electrode on the sample can be either at the bottom (single terminal configuration, Fig.1 (a)), or as a micro-patterned surface electrode (two-terminal configuration, Fig.1 (b) [6]), accessing either bulk or near-surface transport properties.

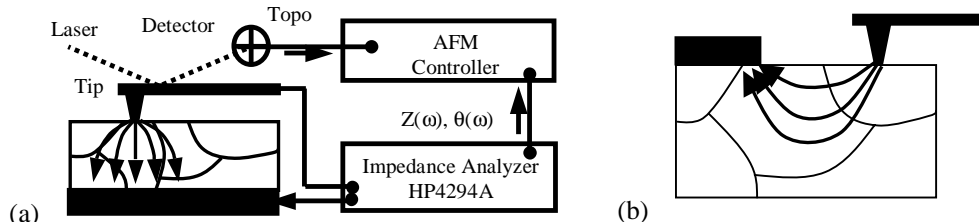


Fig.1 NIM measurements in (a) single terminal and (b) two terminal configuration

(1) Impedance spectroscopy of tip-surface contact

The sample used for the tip-sample contact calibration was a polished $1 \times 2.5 \text{ cm}^2$ copper substrate with a 500nm thick thermally deposited Au layer on top. The single terminal configuration was adopted.

Commercially available gold coated silicon tips (CSC 12 Cr-Au, Micromasch) were used for tip coating quality study. Impedance spectra of a new tip in contact and a damaged tip with Au were collected. To investigate the stray capacitance, platinum coated silicon tips (CSC 12 Pt, Micromasch) with two different cantilever lengths (cantilever A and F) were used. Both cantilevers were brought into contact with Au in the weak indentation regime to minimize the cantilever deformation[5]. The geometries for cantilevers A and F are $(35 \pm 3) \times (110 \pm 5)$ and $(35 \pm 3) \times (250 \pm 5) \mu\text{m}^2$, respectively. The tip height is 15-20 μm . A doped silicon tip (NSC15, Micromasch) and several tips with different coatings: *p*-doped

diamond (DDESP-10), TiN (CSC12 TiN, Micromasch) are chosen for the study of dc bias dependent properties of tip-gold contact.

(2) Impedance imaging and spectroscopy of a ZnO varistor

A polycrystalline ZnO pellet (radius 14 mm, thickness 1.6 mm, grain size $\sim 100\mu\text{m}$) was polished and soldered with In on a copper bottom electrode. For two terminal configurations, 100nm thick Au/NiCr microcontacts were deposited on the polished surface using shadow mask. The bottom electrode configuration was employed for the impedance imaging. Impedance images were acquired using Au coated tip (CSC12 Au A) at tip-sample dc biases of $V_{\text{dc}} = +35\text{V}$ and $+40\text{V}$ and ac probing signal with the frequency = 10kHz and amplitude = 50mV. Impedance spectra were acquire at $V_{\text{dc}} = +20\text{V}$, $+30\text{V}$ and $+40\text{V}$. Prior to and between the measurements, the tip coating quality was tested using the aforementioned calibration method. While the electrical properties of tip-Au and tip-ZnO contacts are different, this procedure ensures that no degradation of the tip coating occurred between successive measurements.

The two-terminal configuration was adopted to study transport in the vicinity of a single grain boundary. One microcontact was electrically connected to the impedance analyzer via a microprobe. Impedance spectra were acquired at $V_{\text{dc}} = +2\text{V}$, $+3\text{V}$ and $+5\text{V}$.

RESULTS AND DISCUSSION

(1) Impedance spectroscopy of tip sample contact

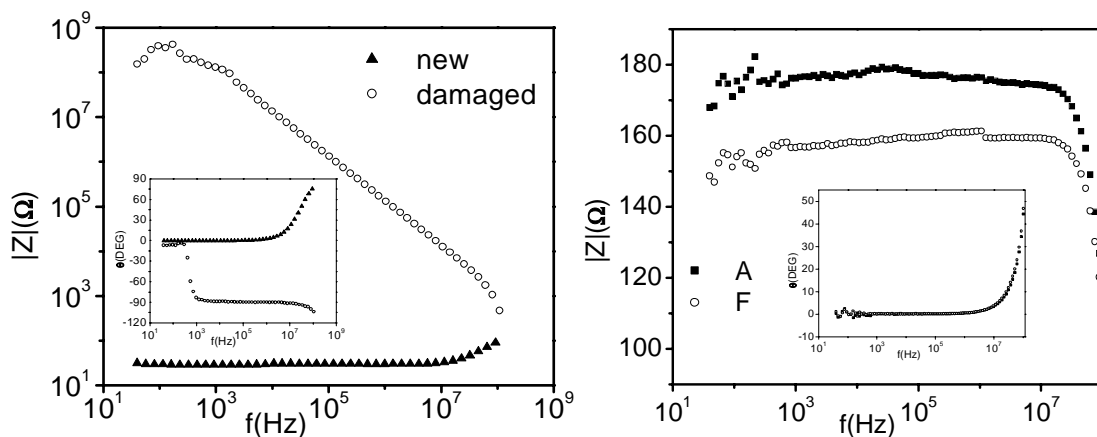


Fig.2. (a) Frequency dependent impedance magnitude for tip-Au contacts for new and damaged tip and (b) different Pt tips in contact with Au surface. Insets show frequency dependence of the phase angle.

From the data (Fig.2 (a)), the phase is virtually 0° over a broad frequency range (40Hz~30MHz), indicative of resistive coupling and thus the contact resistance for a new Au coated tip is $\sim 30\ \Omega$; the tip-surface impedance is bias independent (not shown). For a damaged tip, the contact resistance is much higher ($>100\text{M}\Omega$), and the coupling becomes capacitive, as can be seen from the phase shift to -90° when frequency increases. The contact resistance is strongly bias dependent indicative of a rectifying Schottky contact between Si tip and gold surface.

By fitting the impedance data for two Pt tips with different geometries (Fig.2 (b)) to the L - C - R circuit discussed earlier, contact resistance, stray capacitance and inductance for both cases are determined (Table 1). The capacitance is on the order of 1pF, consistent with previous reports [6]. Note that while the effective areas of the cantilevers A and F differ by a factor of 2, the difference in stray capacitance doesn't exceed 15%, indicating the significant contribution of the tip holder to measured capacitance.

Table 1. Parameters of equivalent circuit for tip-surface contact

Cantilever/Area	Resistance $R(\Omega)$	Capacitance $C(\text{pF})$	Inductance $L(\mu\text{H})$
A ($3850 \mu\text{m}^2$)	176	7.09	0.263
F ($8750 \mu\text{m}^2$)	158	7.90	0.254

While Au and Pt coated tips form ohmic contact with Au, the impedance of a bare silicon tip and TiN, W_2C or diamond coated tips exhibit significant dc bias dependence (Fig.3a). The resistance-voltage characteristics of TiN and diamond tips are almost symmetric, while those of a bare silicon tip is strongly asymmetric, indicating Schottky behavior with subsequent saturation at positive biases and breakdown behavior at negative biases.

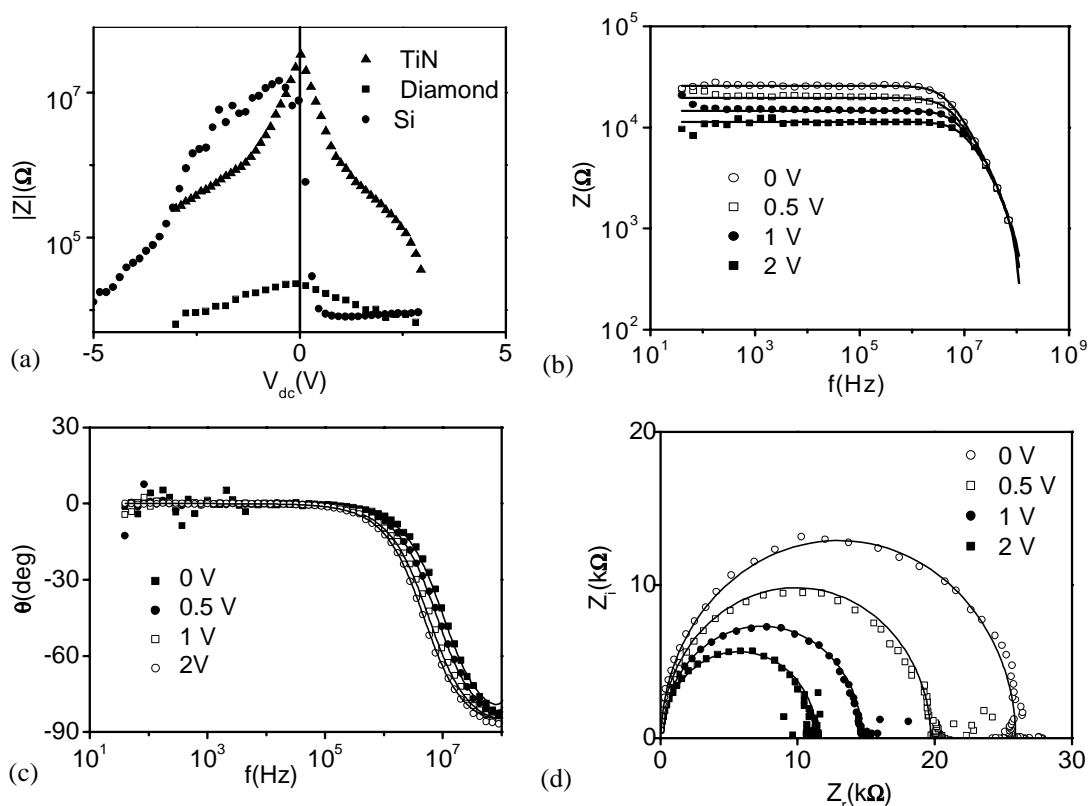


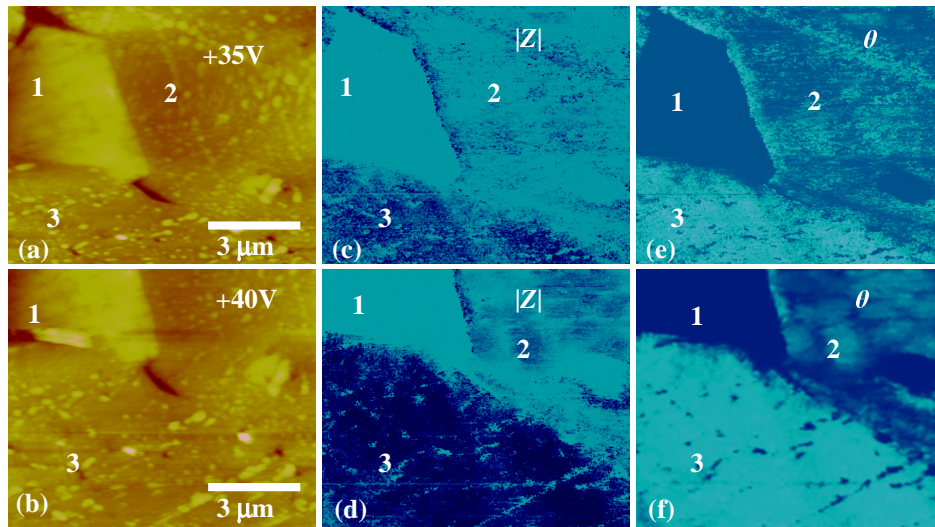
Fig.3. Bias dependence of tip-surface resistance (a) for probes with different coating. Frequency dependence of impedance magnitude (b), phase (c) and Cole-Cole plots (d) for diamond tip-Au contact at different dc biases.

Table 2. Bias dependence of diamond-Au contact characteristics

V_{dc} (volt)	Resistance R(k Ω)	Capacitance C(pF)	Inductance L(μ H)
0	25.89	1.29	0.922
0.5	19.70	1.39	0.919
1.0	14.70	1.35	0.948
2.0	11.40	1.35	0.948

Impedance spectra of the contact between a diamond coated tip and Au at different V_{dc} are shown in Fig.3 b-d. These dependences are well-approximated by the L - C - R equivalent circuit and corresponding parameters are summarized in Table 2. While the contact resistance decreases with dc bias, capacitance and inductance are almost constant

(2) Study of a polycrystalline ZnO varistor

Fig.4 Surface topography (a, b), $|Z|$ (c, d), and θ (e, f) images of ZnO grains at $V_{dc}=35$ V and 40V

Impedance images of three-grain junction in ZnO were acquired at $V_{dc} = +35$ V and +40 (i.e. in the breakdown region) as illustrated in Fig. 4. The phase on grain 1 is -90° , indicating that the transport in this region is restrained and tip-surface coupling is purely capacitive. Impedances in the regions of grains 2 and 3 decrease with tip bias, indicative of the varistor behavior [7].

The Cole-Cole plot of impedance data in the two terminal configuration (tip-electrode separation ~ 50 μ m) exhibits two major relaxation processes as shown in Fig.5. In this case, a pair of parallel R-C elements in series representing the grain boundary and tip/surface Schottky contact provides the best description of the data.

Table 3. Equivalent circuit parameters in two-terminal configuration

V_{dc} (volt)	R_1 (k Ω)	C_1 (pF)	R_2 (k Ω)	C_2 (pF)
2V	194	0.34	125	72
3V	117	0.32	93	74
5V	72	0.33	77	110

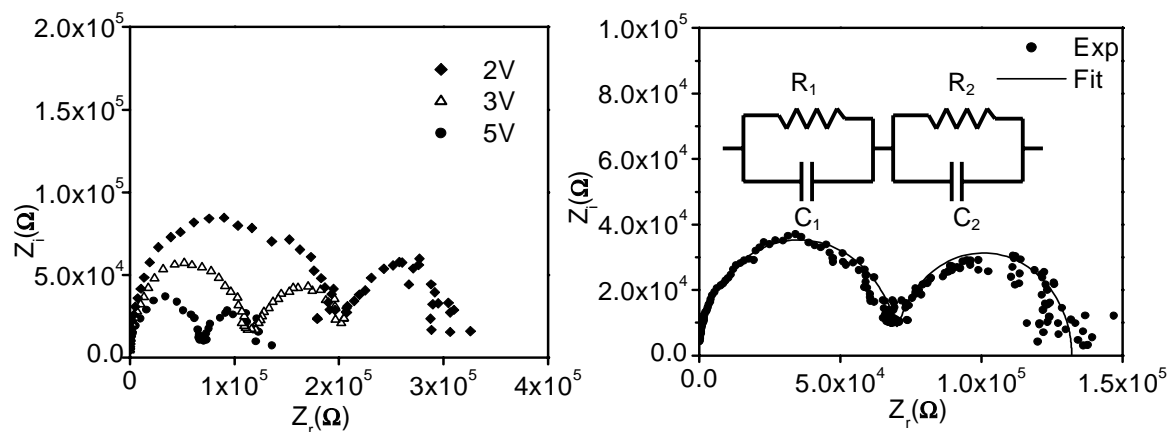


Fig. 5. (a) Cole-Cole plot of impedance data (b) Fitting of the spectrum at $V_{dc}=5V$

From the results in Table 3 and the tip contact measurements the high frequency process (R_1 , C_1) can be associated with the transport through the tip-grain contact and the low frequency process (R_2 , C_2) is related to grain boundary transport. Clearly, positioning of the tip at different distances from the top electrode allows probing the impedance of single grain or several grains (to be reported elsewhere).

CONCLUSION

A scanning probe technique based on the measurement of frequency dependent transport using a conductive AFM tip, referred to as Nanoimpedance Microscopy/Spectroscopy, is developed. The contribution to the electrical transport from various relaxation processes including tip-surface contact can be distinguished based on the analysis of the equivalent circuit. It is applicable for both the spatially resolved study of transport mechanisms of semiconductors and tip-sample contact characterization, thus providing much-needed calibration tool for current based SPMs. This approach is very general and, augmented by the data analysis methods of traditional impedance spectroscopy, can be further extended to examine transport mechanisms in isolated nanoscale systems.

REFERENCES

1. S.V. Kalinin and D.A. Bonnell, in *Scanning Probe Microscopy and Spectroscopy: Theory, Techniques and Applications*, ed. D.A. Bonnell (Wiley VCH, New York, 2000).
2. P. De Wolf, R. Stephenson, T. Trenkler, et al., *J. Vac. Sci. Technol. B* 18, **361** (2000).
3. C.C. Williams, *Annu. Rev. Mat. Sci.* 29, **471** (1999).
4. J.R. Macdonald and W.B. Johnson, in *Impedance Spectroscopy: Emphasizing Solid Materials and Systems*, ed. J.R. Macdonald (Wiley, New York, 1987).
5. David T. Lee and J. P. Pelz, *Rev. Sci. Instrum.*, Vol. 73, **3525** (2002)
6. S.V. Kalinin, Ph.D. Thesis, University of Pennsylvania, Philadelphia, 2002.
7. T. Tran, D. R. Oliver, D. J. Thomson, and G. E. Bridges, *Rev. Sci. Instrum.* **72**, 2618 (2001).
8. L.L. Hench, J.K. West, *Principles of Electronic Ceramics* (Wiley, New York, 1990).